▼ Journal of Research (Science), Bahauddin Zakariya University, Multan, Pakistan.
Vol. 18, No. 1, January 2007, pp. 01-12 ISSN 1021-1012

NUMERICAL SIMULATION OF MAGNETOHYDRODYNAMIC PRESSURE DROP IN A CURVED BEND UNDER DIFFERENT CONDITIONS

Kameel Arshad, Asad Majid
Department of Nuclear Engineering, Pakistan Institute of Engineering and Applied Sciences, Nilore, Islamabad 45650, Pakistan
Muhammad Rafique*, Shahida Jabeen
Department of Physics, University of Azad Jammu and Kashmir, Muzaffarabad 13100, Azad Kashmir, Pakistan
*** email: rafi_722002@yahoo.com**

Abstract
This paper presents a detailed study of liquid-metal flow in a curved bend, under the conditions, when the liquid metal flows first parallel and then perpendicular to the magnetic field, while a constant magnetic field also acts in the transverse direction. The duct has conducting vanadium walls, and liquid metals (lithium, sodium, potassium) have been used as coolants. Magneto hydrodynamic (MHD) equations have been developed in three dimensions in the modified toroidal coordinate system. These coupled sets of equations then have been solved using finite difference techniques and an extended SIMPLER algorithm approach. Calculation of MHD pressure drop has been made for three different liquid metals, lithium, sodium and potassium. The results for curved bend indicate an immense axial MHD pressure drop. The axial MHD pressure drop increases for an increase in both kinds of magnetic field for all three liquid metals. It is found that the MHD pressure drop increases as the liquid metal flows more and more transverse to the magnetic field. The MHD pressure drop is found to be maximum for sodium and minimum for lithium.

Keywords: Curved bend, liquid metals, magneto hydrodynamic (MHD), toroidal.

INTRODUCTION
Liquid metals and its compounds have been proposed as coolants for fusion reactors. They have also been proposed as coolants for limiters and diverters, the high-heat-flux components of a fusion reactor. Because of its reactivity with liquid metals (lithium, sodium, potassium), water is considered a safety risk [Piet

* Corresponding Author 's Address: C/O Shafique General Store, Khan Market, Muzaffarabad, 13100, AzadKashmir, Tel: +923009189301, +925881034691, Fax: +92 51 9223727

1986]. It has been observed that liquid metal flows in high-heat-flux components both transverse to the magnetic field and also from a direction parallel to the magnetic field to a direction perpendicular to the magnetic field. The problem of liquid lithium flow in a straight rectangular duct with conducting walls and transverse magnetic field has been looked at by Kim and Abdou [1989]. The problem of liquid-metal flow in a curved bend where the magnetic field acts in a single transverse direction to the coolant flow for straight duct and curved bend has been looked at by Majid [1999]. However the problem of liquid metal flow in a curved bend when the fluid flows first parallel to the magnetic field and then perpendicular to the magnetic field while a constant magnetic field acts in the transverse direction has not been look at. The knowledge about the MHD pressure drop in this type of magnetic field is however necessary to accomplish a feasible fusion reactor design. A square-cross-section coolant channel was selected for analysis. This channel represents the cooling channel on the face of a limiter or diverter. The channel analyzed would closely resemble the channel on the leading edge of the limiter or diverter [Baker *et al.* 1980]. Fig. 1 shows the geometric configuration of this channel. The coordinate system can be called a modified toroidal coordinate system (Fig. 2) because the cross section of the torus in modified toroidal coordinate system is rectangular while the cross section of the torus in toroidal coordinate system is circular (see Fig. 2).

THE MHD EQUATIONS

The MHD equations, assuming the conditions of steady state, incompressible flow, constant properties, negligible viscous dissipation, and negligible induced magnetic field, are expressed in vector from as follows:

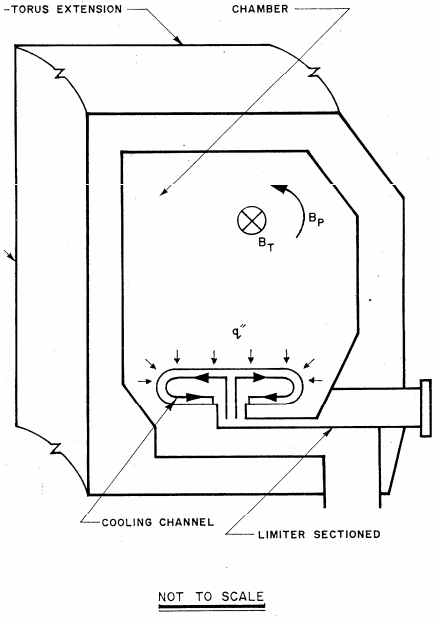

Fig. 1: Geometric Configuration of the Curved Coolant Channel.

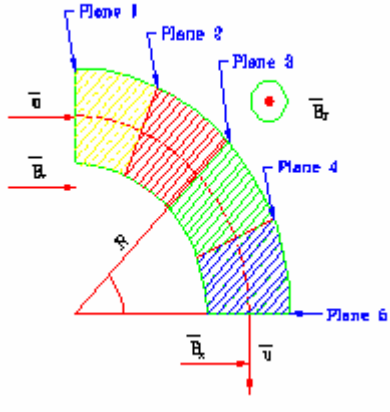

Fig. 2: Geometric Configuration of the Bend.

Continuity:

$$\nabla.u = 0$$

Momentum:

$$\rho(u.\nabla u) = -\nabla P + \mu\nabla.\nabla u + \sigma(-\nabla\phi + u \times B) \times B$$

Ohm's Law:

$$J = \sigma(-\nabla\phi + u \times B),$$

Potential equation:

$$\nabla^2\phi - \nabla.(u \times B) = 0$$

Where B = magnetic field, u = vectorial velocity, ϕ = electrical potential, P = pressure, ρ = fluid density, σ = electrical conductivity, μ = absolute viscosity, J = electrical current.

It has been observed that when liquid metal flows in a duct with conducting walls, the free charge available makes a path through the conducting walls. This current interacts with the magnetic field. If the orientation of the magnetic field is transverse to the flow, then a net force ***(J X B)*** develops, which tends to retard the flow, and thus gives rise to MHD pressure drop. It can be seen from the momentum equation that in MHD flows in the presence of magnetic field, three kinds of fields affect the flow. They are the pressure field, the potential field, and the magnetic field.

The vectorial MHD equations were then expressed in terms of the space variables *x, y,* θ of the modified toroidal coordinate system, with *x* representing distance in the radial direction from the duct centerline, *y* the distance normal to the radial direction, and θ the angle around the loop in the axial direction. The differential equations in terms of the space variables *x, y*, and θ and the major radius are obtained by the use of metric coefficients and are given next (Note that *u* is the velocity in the *x* direction, *v* is the velocity in the *y* direction, and *w* is the velocity in the axial direction):

Continuity:

$$\frac{1}{R+x}\left[\frac{\partial}{\partial x}((R+x)u) + \frac{\partial}{\partial y}((R+x)v) + \frac{\partial}{\partial\theta}(w)\right] = 0,$$

x-momentum:

$$\frac{1}{R+x}\left[\frac{\partial}{\partial x}\left\{(R+x)\rho uu - \mu(R+x)\frac{\partial u}{\partial x}\right\}\right] + \frac{1}{R+x}\left[\frac{\partial}{\partial y}\left\{(R+x)\rho vu - \mu(R+x)\frac{\partial u}{\partial y}\right\}\right]$$

$$+ \frac{1}{R+x}\left[\frac{\partial}{\partial\theta}\left\{\rho wu - \frac{\mu}{(R+x)}\frac{\partial u}{\partial\theta}\right\}\right] = -\frac{\partial P}{\partial x} + \frac{\rho ww}{(R+x)} - \frac{2\mu}{(R+x)(R+x)}\frac{\partial w}{\partial\theta}$$

$$- \frac{\mu\mu}{(R+x)(R+x)} + \sigma B_\theta wB_x - \sigma B_\theta B_\theta u - \sigma B_\theta\frac{\partial\phi}{\partial y} - \sigma uB_yB_y + \sigma B_yB_x v + \sigma\frac{B_y}{(R+x)}\frac{\partial\phi}{\partial\theta},$$

y-momentum:

$$\frac{1}{R+x}\left[\frac{\partial}{\partial x}\left\{(R+x)\rho uv - \mu(R+x)\frac{\partial v}{\partial x}\right\}\right] + \frac{1}{R+x}\left[\frac{\partial}{\partial y}\left\{(R+x)\rho vv - \mu(R+x)\frac{\partial v}{\partial y}\right\}\right]$$

$$+ \frac{1}{R+x}\left[\frac{\partial}{\partial\theta}\left\{\rho wv - \frac{\mu}{(R+x)}\frac{\partial v}{\partial\theta}\right\}\right] = -\frac{\partial P}{\partial y} + \sigma B_\theta wB_y - \sigma B_\theta B_\theta v + \sigma B_\theta\frac{\partial\phi}{\partial x}$$

$$+ \sigma uB_yB_x - \sigma B_xB_x v - \sigma\frac{B_x}{(R+x)}\frac{\partial\phi}{\partial\theta},$$

θ-momentum:

$$\frac{1}{R+x}\left[\frac{\partial}{\partial x}\left\{(R+x)\rho uw-\mu(R+x)\frac{\partial w}{\partial x}\right\}\right]+\frac{1}{R+x}\left[\frac{\partial}{\partial y}\left\{(R+x)\rho vw-\mu(R+x)\frac{\partial w}{\partial y}\right\}\right]$$

$$+\frac{1}{R+x}\left[\frac{\partial}{\partial \theta}\left\{\rho ww-\frac{\mu}{(R+x)}\frac{\partial w}{\partial \theta}\right\}\right]=-\frac{1}{R+x}\frac{\partial P}{\partial \theta}-\frac{\rho uw}{(R+x)}+\frac{2\mu}{(R+x)(R+x)}\frac{\partial u}{\partial \theta}$$

$$-\frac{\mu w}{(R+x)(R+x)}+\sigma B_\theta vB_y-\sigma B_y B_y w-\sigma B_y\frac{\partial \phi}{\partial x}-\sigma wB_x B_x+\sigma B_\theta B_x u+\sigma B_x\frac{\partial \phi}{\partial y},$$

Potential equation

$$\frac{1}{R+x}\left[\frac{\partial}{\partial x}\left((R+x)\frac{\partial \phi}{\partial x}\right)+\frac{\partial}{\partial y}\left((R+x)\frac{\partial \phi}{\partial y}\right)+\frac{\partial}{\partial \theta}\left(\frac{1}{(R+x)}\frac{\partial \phi}{\partial \theta}\right)\right]$$

$$=-\frac{1}{(R+x)}\left[\frac{\partial}{\partial x}((R+x)(vB_\theta-wB_y))+\frac{\partial}{\partial y}((R+x)(wB_x-uB_\theta))+\frac{\partial}{\partial \theta}(uB_y-vB_x)\right]$$

METHOD OF SOLUTION

The differential equations described above were solved using the finite difference techniques described by Patankar [1979a,b, 1980], Patankar and Spalding [1970, 1972a,b, 1974a,b, 1978]. The new computer code SIMPLMHD was upgraded to incorporate the three different liquid metal properties at 230^{0}C [Holman 1976, Mantell 1958]. This code incorporates the extended SIMPLER method [Majid 1990] for solving the coupled set of MHD equations.

The discretization equations were developed using the control volume approach [Patankar 1980]. The numerical scheme used was the power law scheme. The potential equation is solved by ordinary finite difference techniques [Majid 1990]. The final discretization equations, where the magnetic field is assumed to operate in the x-θ plane as well as in the y direction are obtained as follow:

x-momentum:

$$u_p(a_T+a_B+a_N+a_S+a_E+a_W)=a_Tu_T+a_Bu_B+a_Nu_N+a_Su_S+a_Eu_E+a_Wu_W$$

$$+\left[\frac{\rho ww}{(R+x)}\right]_P-2\mu\left[\frac{w}{(R+x)}\right]_t\Delta x\Delta y+2\mu\left[\frac{w}{(R+x)}\right]_b\Delta x\Delta y-\left[\frac{\mu u}{(R+x)(R+x)}\right]_P\Delta V$$

$$-\left[P_e-P_w\right]\delta A(x)+\left[\sigma B_\theta B_x w\right]_p\Delta V-\left[\sigma B_\theta B_\theta u\right]_p\Delta V-\left[\sigma B_\theta(R+x)\phi\right]_n\Delta\theta\Delta x+\left[\sigma B_\theta(R+x)\phi\right]_s\Delta\theta\Delta x$$

$$-\left[\sigma B_y B_y u\right]_p\Delta V+\left[\sigma B_y B_x v\right]_p\Delta V+\left[\sigma B_y\phi\right]_n\Delta x\Delta y-\left[\sigma B_y\phi\right]_S\Delta x\Delta y$$

where ΔV= volume of control volume, P = location of grid point of interest ,

n = northern face of control volume, s = southern face of control volume,
e = eastern face of control volume, w = western face of control volume,
t = top face of control volume, b = bottom face of control volume,
W, E = location of the neighboring points in the x direction,
S, N= location of the neighboring points in the y direction,
B, T= location of the neighboring points in the θ direction,
δA (x) = area of the control volume face perpendicular to x-direction,

And

$$a_T = D_t A(|P_t|) + [|-F_t, 0|]\ ; \qquad a_B = D_b A(|P_b|) + [|F_b, 0|]\ ;$$
$$a_N = D_n A(|P_n|) + [|-F_n, 0|]\ ; \qquad a_S = D_s A(|P_s|) + [|F_s, 0|]\ ;$$
$$a_E = D_e A(|P_e|) + [|-F_e, 0|]\ ; \qquad a_W = D_w A(|P_w|) + [|F_w, 0|];$$
$$a_p = a_T + a_B + a_N + a_S + a_E + a_W$$
$$D_t = \frac{\mu}{((R+x)d\theta)|_t}\Delta x\Delta y\ ; \qquad D_b = \frac{\mu}{((R+x)d\theta)|_b}\Delta x\Delta y\ ;$$
$$D_n = \frac{\mu(R+x)|_n \Delta x\Delta\theta}{\delta y_n}\ ; \qquad D_s = \frac{\mu(R+x)|_s \Delta x\Delta\theta}{\delta y_s}$$
$$D_e = \frac{\mu(R+x)|_e \Delta y\Delta\theta}{\delta y_e}\ ; \qquad D_w = \frac{\mu(R+x)|_w \Delta y\Delta\theta}{\delta y_w}$$
$$P_e = \frac{F_e}{D_e};\ P_w = \frac{F_w}{D_w};\ P_n = \frac{F_n}{D_n};\ P_s = \frac{F_s}{D_s};\ P_t = \frac{F_t}{D_t};\ P_b = \frac{F_b}{D_b};$$
$$F_e = (R+x)\rho u|_e \Delta y\Delta\theta\ ; \qquad F_w = (R+x)\rho u|_w \Delta y\Delta\theta\ ;$$
$$F_n = (R+x)\rho v|_n \Delta x\Delta\theta\ ; \qquad F_s = (R+x)\rho v|_s \Delta x\Delta\theta\ ;$$
$$F_t = (R+x)\rho w|_t \Delta y\Delta x\ ; \qquad F_b = (R+x)\rho w|_b \Delta y\Delta x\ ;$$
$$A(|P|) = [|0, (1-0.1|P|)^5|]$$

Operator $[|C, K|]$=the greater of C, K [Holman 1976],

$\Delta x, \Delta y, \Delta\theta$ =dimensional parameters of the control volume,

$w|_b$ =calculation of the w velocity at the corresponding location of the bottom face of the control volume and similarly for others with this notation.

$\delta x, \delta y, \delta z$ = distance between the grid points in the *x, y* and *z* directions, respectively.

***y*-momentum**

$$w_p(a_T + a_B + a_N + a_S + a_E + a_W) = a_T w_T + a_B w_B + a_N w_N + a_S w_S + a_E w_E + a_W w_W$$
$$-[P_n - P_s]\delta A(y) - [\sigma B_\theta B_\theta \upsilon]_p \Delta V + [\sigma B_y B_\theta w]_p \Delta V - [\sigma B_x B_x \upsilon]_p \Delta V + [\sigma B_y B_x u]_p \Delta V$$
$$+[\sigma B_\theta (R+x)\phi]_e \Delta\theta\Delta y - [\sigma B_\theta (R+x)\phi]_w \Delta\theta\Delta y - \sigma((B_x\phi|_t))\Delta x\Delta y + \sigma((B_x\phi|_b))\Delta x\Delta y$$

where the coefficients of the discretization equation and the nomenclature are the same as the coefficients and nomenclature for the x-momentum equation except that now they pertain to the control volume around the *v* velocity.

θ-momentum;

$$w_p(a_T+a_B+a_N+a_S+a_E+a_W)=a_T w_T+a_B w_B+a_N w_N+a_S w_S+a_E w_E+a_W w_W$$
$$-\left[\frac{\rho wu}{R+x}\right]_P \Delta V+2\mu\left[\frac{u}{R+x}\right]_t \Delta x\Delta y-2\mu\left[\frac{u}{R+x}\right]_b \Delta x\Delta y-\left[\frac{wu}{(R+x)(R+x)}\right]_P \Delta V$$
$$-\left[P_t-P_b\right]\delta A(z)+\left[\sigma B_\theta B_y v\right]_P \Delta V-\left[\sigma B_y B_y w\right]_P \Delta V-\left[\sigma B_y (R+x)\phi\right]_e \Delta\theta\Delta y+\left[\sigma B_y (R+x)\phi\right]_w \Delta\theta\Delta y$$
$$+\left[\sigma B_\theta B_x u\right]_P \Delta V-\left[\sigma B_x B_x w\right]_P \Delta V+\left[\sigma B_x (R+x)\phi\right]_n \Delta\theta\Delta x-\left[\sigma B_x (R+x)\phi\right]_s \Delta\theta\Delta x$$

where the coefficients of the discretization equation and the nomenclature are the same as the coefficients and nomenclature for the x-momentum equation except for the pertain to the control volume around the *w* velocity.

Potential equation:

$$a_P\phi_P=a_E\phi_E+a_W\phi_W+a_N\phi_N+a_S\phi_S+a_T\phi_T+a_B\phi_B-\left(((R+x)(vB_\theta-wB_y))\big|_e\right)\Delta y\Delta\theta$$
$$+\left(((R+x)(vB_\theta-wB_y))\big|_w\right)\Delta y\Delta\theta+\left(((R+x)(wB_x-uB_\theta))\big|_n\right)\Delta x\Delta\theta$$
$$-\left(((R+x)(wB_x-uB_\theta))\big|_s\right)\Delta x\Delta\theta+\left((uB_y-vB_x)\big|_t-(uB_y-vB_x)\big|_b\right)\Delta y\Delta x,$$

where

$$a_E=\frac{(R+x)\big|_e}{\delta x_e}\Delta y\Delta\theta; \qquad a_w=\frac{(R+x)\big|_w}{\delta x_w}\Delta y\Delta\theta;$$
$$a_N=\frac{(R+x)\big|_n}{\delta x_n}\Delta x\Delta\theta; \qquad a_S=\frac{(R+x)\big|_s}{\delta x_s}\Delta x\Delta\theta;$$
$$a_T=\frac{1}{(R+x)\big|_t}\frac{1}{\delta\theta_t}\Delta x\Delta y; \qquad a_B=\frac{1}{(R+x)\big|_b}\frac{1}{\delta\theta_b}\Delta x\Delta y;$$
$$a_P=a_E+a_W+a_N+a_S+a_T+a_B$$

The definition of various control volume parameters is the same as given for the x-momentum equation, only now they pertain to the control volume around the potential.

The boundary conditions for solving the momentum equations evolve from the "no slip condition" where the velocities *u, v,* and *w* are zero at the wall. The boundary condition to solve the potential equation is the "thin wall boundary condition" where the walls are thin enough that current cannot flow in a direction in which the wall is thin but can flow only in the direction along which walls extend. The significant feature of these analyses was the development of the pressure equation by combining continuity and discretized momentum equations. The final set of equations to be solved consisted of three discretized momentum equations for three velocities *u, v,* and *w;* one pressure equation; and one electric potential equation.

The first step according to the SIMPLER algorithm was to guess a velocity field. An electric potential field was also guessed. The magnetic field was given. The various steps of the SIMPLER algorithm were then followed until a converged velocity field and pressure field were obtained. With the newly achieved converged velocity field and pressure field, the potential equation was solved and a potential field was obtained. With the newly obtained velocity field, pressure field, and electric potential field, the whole procedure was repeated; i.e., the various steps of the SIMPLER algorithm were followed where in place of guessed fields newly calculated fields were used. This procedure was repeated until a converged electric potential field along with a velocity field and a pressure field was obtained.

ANALYSIS OF FLOW IN A CURVED BEND

The computer code SIMPLMHD was written, as mentioned earlier in such away that results can be obtained for two geometries, a straight duct and a curved bend, by controlling the major radius R. The exit condition of the flow was considered as fully developed. As the length of the bend under consideration is not sufficient for the flow to become fully developed, the specification of the exit condition needs justification. The justification is that the Peclet number for axial flow is sufficiently large (Peclet number> 100) thus the flow conditions downstream at the exit will not significantly affect the flow conditions upstream at the exit.[4-12] The assumption of fully developed conditions at the exit will thus not cause any significant error in the analysis. It was assumed that at the inlet, the flow enters with a three dimensional parabolic velocity profile. The assumption in the inlet profile is not expected to drastically effect our calculations as we start measuring the pressure from the plane next to the inlet plane. It has to be noted that the magnetic field force affecting the flow is so strong as compared with the ordinary hydrodynamic forces that the flow takes up the magnetic effects within a very small distance from the inlet. This can be seen from the ordinary hydrodynamic pressure drop, which is only about 400 pa m^{-1} as compared with the MHD pressure drop, whose minimum value is about 20000 pa m^{-1} and soars above this value as magnetic field strength is increased. Thus any error because of an inlet profile assumption is expected to be nulled out within the movement of the fluid from the first inlet plane to the second plane in the direction of the flow.

In these analyses, because of the limitation of computational power available, the grid considered was 5 X 5 on the cross section and 5 planes downstream. The dimensions of the channel analyzed were 1 cm X 1 cm. The bend analyzed had a radius of 5 cm. The magnetic field in the x direction and y direction are considered to be constant. The wall thickness was taken to be 1mm. The flow was analyzed at a Reynolds number of 5276 for lithium, 13928 for sodium and 16411 for potassium. The Hartmann number M for the flow, defined as $M=Ba\sqrt{(\sigma/\mu)}$, where "a" is dimension of duct, "σ" is the electrical conductivity of the fluid, and μ is the absolute viscosity of the fluid. The Hartmann number for maximum magnetic field in different planes is given in the Table 1.

The calculation of the pressure gradient (Pascal per meter) in a 5-cm-radius bend when magnetic field acts in x, y and θ directions, was performed. The results are shown in Figs 3 to 8. The pressure gradient along the curved bend for

different values of constant magnetic field in x-θ plane and different values of constant magnetic field in y direction are shown in from Figs 3 and 4 for lithium.

Table 1: Hartmann number for maximum magnetic field in different planes.

Liquid Metal	Plane	Magnetic Field (Tesla)	Hartmann Number
Lithium	x-θ plane	0.50	1517
	x-y plane	0.40	1214
Sodium	x-θ plane	0.35	2321
	x-y plane	0.40	2653
Potassium	x-θ plane	0.45	2666
	x-y plane	0.40	2370

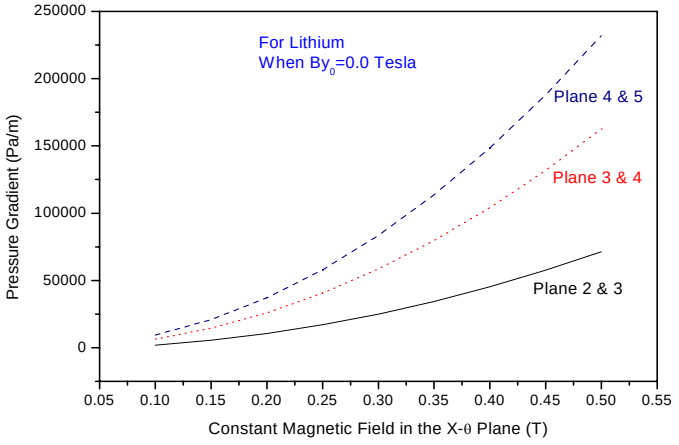

Fig. 3: This is the case of curved bend for lithium, where the flow is first parallel and then perpendicular to the magnetic field in x direction, the y transverse direction magnetic field is also exists. For this case By_0 = 0.0 Tesla.

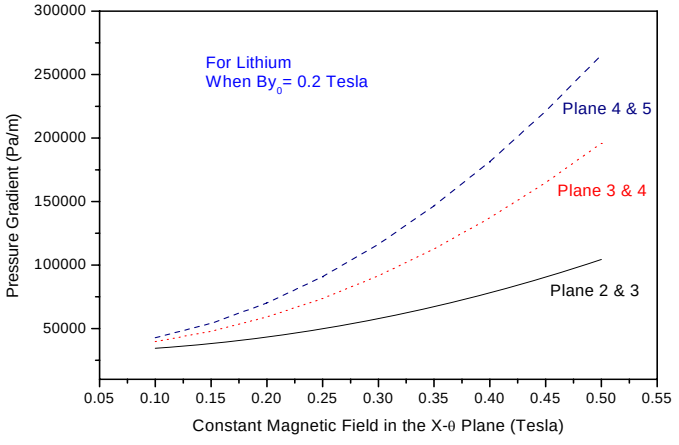

Fig. 4: This is the case of curved bend for lithium, where the flow is first parallel and then perpendicular to the magnetic field in x direction, the y transverse direction magnetic field is also exists. For this case By_0 = 0.2 Tesla.

The MHD pressure drop is found maximum between 4 & 5 plane. It is found that MHD pressure drop increases for an increase in magnetic field in the x-θ plane and also increases for an increase in magnetic field in y direction.

The pressure gradient along the curved bend for different values of constant magnetic field in x-θ plane and different values of constant magnetic field in y direction are shown in from Figs 5 and 6 for sodium.

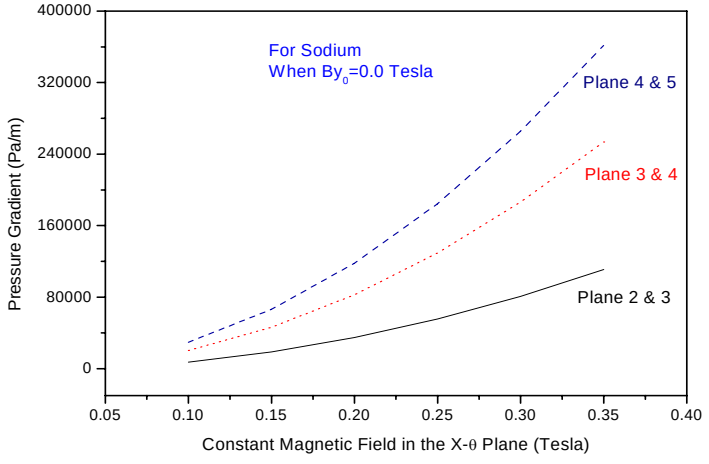

Fig. 5: This is the case of curved bend for sodium, where the flow is first parallel and then perpendicular to the magnetic field in x direction, the y transverse direction magnetic field is also exists. For this case By_0 = 0.0 Tesla.

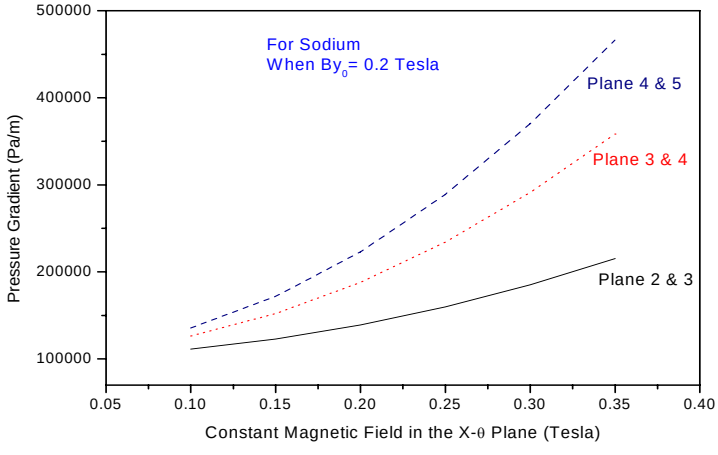

Fig. 6: This is the case of curved bend for sodium, where the flow is first parallel and then perpendicular to the magnetic field in x direction, the y transverse direction magnetic field is also exists. For this case By_0 = 0.2 Tesla.

The MHD pressure drop is found maximum between 4 & 5 plane. It is found that MHD pressure drop increases for an increase in magnetic field in the x-θ plane and also increases for an increase in magnetic field in y direction.

The pressure gradient along the curved bend for different values of constant magnetic field in x-θ plane and different values of constant magnetic field in y direction are shown in from Figs 7 and 8 for potassium. The MHD pressure drop is found maximum between 4 & 5 plane. It is found that MHD pressure drop increases for an increase in magnetic field in the x-θ plane and also increases for an increase in magnetic field in y direction. It can be seen very clearly that MHD pressure drop is maximum for sodium and minimum for lithium.

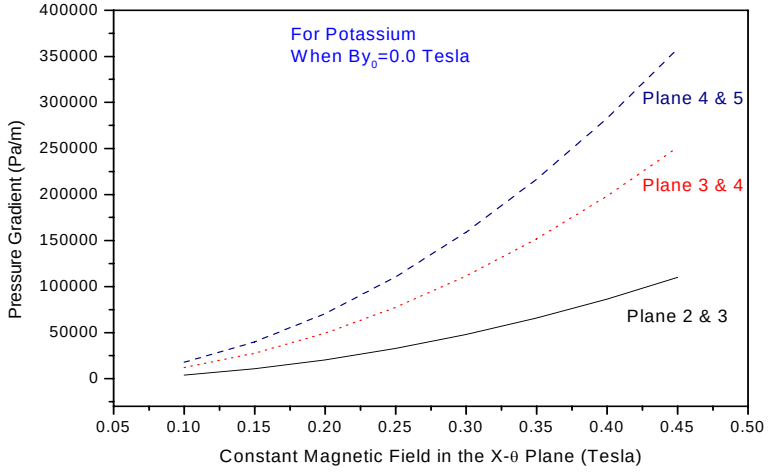

Fig. 7: This is the case of curved bend for potassium, where the flow is first parallel and then perpendicular to the magnetic field in x direction, the y transverse direction magnetic field is also exists. For this case By_0= 0.0 Tesla.

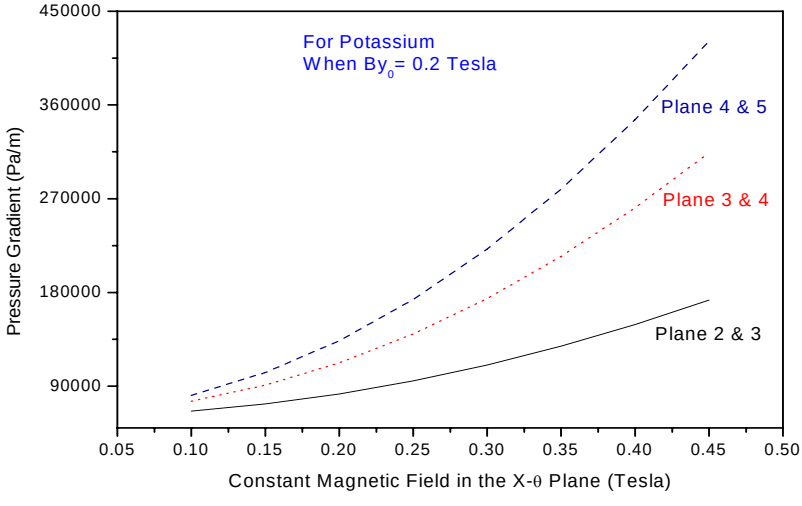

Fig. 8: This is the case of curved bend for potassium, where the flow is first parallel and then perpendicular to the magnetic field in x direction, the y transverse direction magnetic field is also exists. For this case By_0 = 0.2 Tesla.

CONCLUSIONS AND DISCUSSION

The calculation of magnetohydrodynamic (MHD) pressure drop has been made when liquid metal flows first parallel and then perpendicular to the magnetic field. It is observed that the MHD pressure drop increases as fluid flows more and more transverse to the applied magnetic plane in the x-θ plane. This behavior has been observed for all three liquid metals, lithium, sodium, and potassium. In the second stage of analysis a constant magnetic field in the y-direction, which is basically transverse to the fluid flow at all points, was also applied along with the constant magnetic field in the x-θ plane. The three fluids depicted the same behavior only the magnitude of MHD pressure drop was more primarily because of the transverse magnetic field. These analyses indicate that in the magnetic field environment considered lithium still remains the best coolant for high heat flux components of a fusion reactor from MHD pressure drop point of view.

References

Baker, C.C. *et al*., (**1980**) STARFIRE, ANL/FPP-80-1.

Holman, J.P. (**1976**) "Heat Transfer", 4th edn, McGraw-Hill Kogakusha Ltd. Tokyo

Kim, C.N. and Abdou, M.A. (**1989**) "Numerical Method for Fluid Heat Flow and Heat Transfer in Magnetohydrodynamic Flow", *Proceedings of 10th Topological Meeting on Technology of Fusion Energy*, Salt Lake City Utah.

Majid, A. (**1990**) "Use of Liquid Metals for Cooling High Heat Flux Components of a Fusion Reactor", PhD Thesis, University of California, Los Angeles.

Majid, A. (**1999**) "Magnetohydrodynamic pressure Drop in a Straight Duct and a Curved Bend in the Presence of Transverse Magnetic Field and Gravity Field" Fusion Technology, Vol. 36.

Mantell, C.L. (**1958**) "Engineering Materials Handbook" 1st edn, McGraw-Hill Book Company, New York, Toronto, London.

Patankar, S.V. (**1979a**) "A Calculation Procedure for Two-Dimensional Elliptical Situation", Numerical Heat Transfer, Vol. 2.

Patankar, S.V. (**1979b**) "The Concept of the Fully Developed Regime in Unsteady Heat Conduction, in: J.P. Hartnet, T.F. Irvine, Jr., Pferder, E. and Spawarrow, E.M. (Eds.), *Studies in Heat Transfer*, Hemisphere, Washington, D.C.

Patankar, S.V. (**1980**) "Numerical Heat Transfer and Fluid Flow", Hemisphere Publishing Corporation, New York.

Patankar, S.V. and Spalding, D.B. (**1970**) " Heat and Mass Transfer in Boundary Layers", 2nd edn., Intertext, London.

Patankar, S.V. and Spalding, D.B. (**1972a**) “A Calculation Procedure for Heat Mass and Momentum Transfer in 3-Dimensional Parabolic Flows”, *Int. J. Heat Mass Transfer*, **15**, 1787.

Patankar, S.V. and Spalding, D.B. (**1972b**) “A Computer modal for 3-Dimensional Flows in furnaces”, Proceedings of 14th Symposium (Int.) on Combustion, The Combustion Institute, p. 605.

Patankar, S.V. and Spalding, D.B. (**1974a**) “A Calculation Procedure for the Transient and Steady state Behavior of Shell and Tube Heat Exchanger”, In: *Heat Exchanger: Design and Theory Source Book*, Hemisphere, Washington, D.C.

Patankar, S.V. and Spalding, D.B. (**1974b**) “Simultaneous Predictions of Flow Pattern and Radiation for 3- Dimensional Flames”, In: *Heat Transfer in Flames*, Hemisphere, Washington, D.C.

Patankar, S.V. and Spalding, D.B. (**1978**) “Computer Analysis of the 3-Dimensional Flow and Heat Transfer in Stream Generator, *Forsch. Ingenieurwes,* **44**, 47.

Piet, S.J. (**1986**) “Common Views of Potentially Attractive Fusion Concept”, *Proceedings of 7th Topological Meeting on Technology of Fusion Energy*, Reno, Nevada.